Available online at www.sciencedirect.com

ScienceDirect

Procedia CIRP 108 (2022) 543–548

www.elsevier.com/locate/procedia

6th CIRP Conference on Surface Integrity

Surface integrity of new dry-electropolishing technology on WC-Co cemented carbides

Guiomar Riu[a,b,*], Dominik Weil[c], Luis Llanes[b], Kurt E. Johanns[d], Warren C. Oliver[d], Joan Josep Roa[a]

[a]*Steros GPA Innovative S.L.U., Maracaibo 1, Barcelona 08030, Spain*
[b]*Department of Materials Science and Engineering - Universitat Politècnica de Catalunya (EEBE), Eduard Maristany 16, Barcelona 08019, Spain*
[c]*KLA-Tencor GmbH, Moritzburger Weg 67, Dresden 01109, Germany*
[d]*KLA-Corporation, 105 Meco Lane, Oak Ridge 37830, USA*

* Corresponding author. Tel.: +34-931-256-536; *E-mail address:* g.riu@gpainnova.com

Abstract

This study is focused on WC-Co dry-electropolished by DryLyte® technology that allows to obtain corrosion-free surfaces with a roughness below 9 nm. The main goal behind this research is to investigate the surface integrity trying to correlate the remanent microstructure after different dry-electropolishing times as a function of the hardness and elastic modulus evolution though massive nanoindentation. The quality of the surface has been evaluated by using advanced characterization techniques and the mechanical response treated by using the statistical methodology proposed by Ulm and Constantinides. To sum up, a close correlation is observed between the residual microstructure and the surface integrity in terms of hardness and elastic modulus maps.

Keywords: WC-Co hardmetal; DryLyte® technology; Surface integrity

1. Introduction

Cemented carbides, also known as hardmetal (WC-Co), is a heterogeneous composite material constituted by ceramic particles united with a metallic cobalt (Co) binder. The combination of these two interlinked phases provides the material with excellent mechanical properties. In this sense, the ceramic particles enhance hardness and wear resistance while the metallic Co binder improves the fracture toughness. As a consequence, the range of applications is extremely wide, such as cutting tools and structural components among others [1].

In fact, WC-Co carbides are used to be employed as cutting tools, where typically diamond grinding as a post processing technique is required. This process modifies the surface integrity of the material inducing mainly compressive residual stresses, microcracks and/or nanometric cavities mainly located at the interphase between both constitutive phases. In addition, grinding process promotes phase transformation of the metallic Co binder, from face-centered cubic (fcc) to hexagonal-close packed (hcp) [2,3].

For some applications it is important to maintain the surface compressive residual stresses induced by the as-built process of the parts, since they are responsible for enhancement of the fatigue behaviour, wear resistance and fracture strength of the material [4]. However, in some cases polishing process after grinding are required, since the roughness level achieved ranges between hundreds of nanometers up to several tens of micrometers, affecting post-processing techniques like the deposition process.

2212-8271
10.1016/j.procir.2022.03.085

In the current industry, conventional polishing techniques are being implemented, such as chemical, mechanochemical and electrochemical polishing among others in order to reach the desired requirements in terms of superficial roughness. However, depending on the media employed, it is possible to corrode the metallic Co binder and/or produce an embrittlement of the WC particles as found in [5-8]. Mainly, the information found in the literature, show a clear tendency for the metallic Co binder to undergo corrosion in contact with acidic or even neutral media (pH≤7), decreasing mechanical and tribological properties under service-like working conditions.

In order to avoid corrosion in the metallic Co binder provided by the different media employed during the conventional polishing techniques, the DryLyte® technology with a suitable electrolyte has been used in this study. This technology uses a resin of ionic exchange with a spherical non-conductive solid electrolyte. These particles are a copolymer with a macroporous structure that allows retaining inside the desired media, improving the electrical conductivity between them. DryLyte® produces a layer-by-layer removal of the material due to the spherical electrolyte particle only interacts with the peaks of the roughness, achieving a selective smoothing of the surface. In this sense, this technology leads to achieve the desired roughness by removing the minimum amount of material. Electrical parameters applied are a combination of direct and alternating current which promote the oxidation and solubility of the polished surface [9].

Whitin this context, this study aims to correlate the remanent microstructure after different dry-electropolishing times by using the DryLyte® technology as a function of the mechanical surface integrity in terms of hardness and elastic modulus cartography maps. In doing so, the mechanical integrity has been evaluated at the submicrometric length scale by means of nanoindentation technique. The surface quality after each polishing steps has been evaluated in terms of microstructure, damage and superficial roughness by using advanced characterization techniques.

2. Experimental procedure

Samples investigated in this study are a commercial grade of WC-Co with a 10% of the metallic Co binder, post-processed with grinding technique.

Prior the microstructural and superficial integrity evaluation as a function of the different polishing steps; a commercial ground WC-Co grade was polished by using the DryLyte® technology at 5, 15 and 30 min. A non-polished specimen (labeled as as-received material, AR) has been also used as a reference, where the damage induce during the grinding process is maximum.

The microstructural parameters were evaluated by using advanced characterization techniques. In this regard, the roughness evolution was measured by Laser Scanning Confocal Microscopy (LSCM, Sensofar Metrology) using a cut-off value of 0.8 μm. Microstructure evolution were evaluated by Field Emission Scanning Electron Microscopy (FESEM, Carl Zeiss Neon 40) while the sub-superficial microstructure though cross-section by using focused ion beam (FIB, Carl Zeiss Neon 40) and subsequently FESEM inspection. A Ga^+ ion source was used to mill the surface at a voltage of 30 kV. The polishing process was conducted in two different steps; initially at a high current of 10 nA and subsequently a fine polishing process performed at a current of 500 pA and 30 kV acceleration voltage.

Hardness (H) and elastic modulus (E) cartography maps at the submicrometric length scale, for each investigated condition, were determined by means of the nanoindentation technique by using the Oliver and Pharr method [10,11]. The different cartography maps were performed with an iNano from KLA-Tencor unit, equipped with a sharp Berkovich diamond tip indenter. An homogeneous array of a 2,500 imprints (50 by 50) were performed per specimen under load control mode at 25 mN of maximum applied load into surface. The distance between imprints was kept constant at 2 μm (10 times the maximum displacement into surface in concordance with the information reported in [12,13]), in order to avoid any overlapping effect. Strain rate was held constant at 0.05 s^{-1} and the indenter shape was carefully calibrated for true indentation depth as small as 20 nm by indentating on standard Fused Silica material with a well-known Young's modulus of 72 GPa [10].

3. Results and discussions

3.1. Microstructural inspection

Before evaluate the microstructural evolution in front of dry-electropolishing time, the main microstructural parameters for the investigated WC-Co grade were measured (summarized in Table 1). Mean grain size (d_{WC}) was calculated following linear intercept method (LIM) by using at least five FESEM micrographs polished during 30 min (see Fig. 1). Contiguity (C_{WC}), binder content (V_{binder}) and mean free path (λ_{binder}) were estimated with empirical relations [14-16].

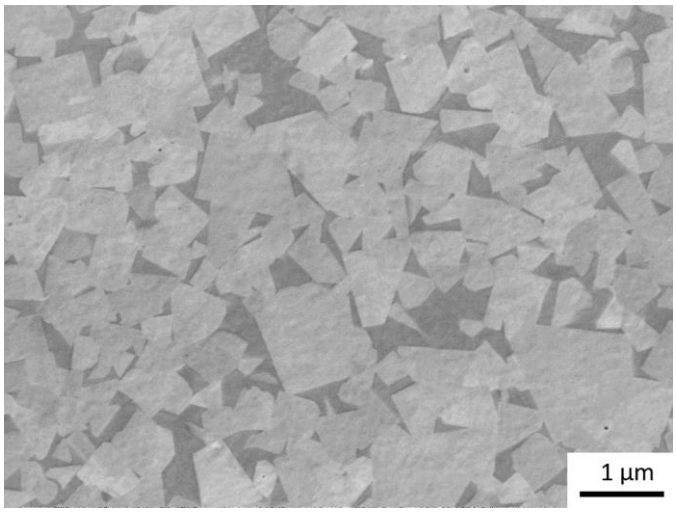

Fig. 1. FESEM micrograph of WC-Co grade after being polished by using the DryLyte® technology for 30 min.

Table 1. Summary of the main microstructural parameters of the WC-Co grade investigated here.

d_{WC} (μm)	C_{WC}	V_{binder} (%)	λ_{binder} (μm)
1.91 ± 0.29	0.56 ± 0.10	10	0.50 ± 0.12

Fig. 2 shows the microstructure evolution of the specimen with different polishing times (from AR up 30 min). As it can be observed, while dry-electropolishing time increases the damage induced during the grinding process (Fig. 2b) progressively disappears, allowing to show the WC-Co microstructure.

Previous studies had evaluated the thickness of the surface damaged by grinding process, obtaining a layer ranged between 200 to 400 nm of pulverized WC grains with smeared Co phase [4]. As DryLyte® process removes material selectively (from top to bottom), the electrolyte reacts by removing the peaks of the ground microstructure and subsequently layer by layer removing the deformed layer until reach practically the WC-Co microstructure free of defects and with a Ra of around 20 nm as shown in Fig. 2a. As it is shown in this image, the roughness evolution as a function of time drops considerable during the first 15 min where the maximum difference between peaks and valleys are. In addition, associated error of roughness measurements decreases as the surface becomes smoother, yielding a qualitative information about the planarity of the obtained specimen. This is in concordance with the FESEM evolution micrographs where is clearly visible that the scratches induced during the grinding process decreases as the polishing time increases.

Furthermore, in order to evaluate the final microstructure achieved with DryLyte® technology, FIB cross-section had been conducted in 30 min polished sample (see dash area in Fig. 2e). Fig. 3 shows the subsequently FESEM inspection where a heterogeneous microstructure is evident. In some regions, grinding effect is still present while in other regions the planarity between both constitutive phases (WC/Co) and/or between different crystallographic orientation for the WC particles are achieved. In that sense, DryLyte® technology does not induce leaching on the metallic Co binder and/or WC embrittlement.

3.2. Mechanical properties

Fig. 4a and 4b shows the nanoindentation hardness and elastic modulus as a function of the difference polished times investigated here, respectively. As it can be seen, the associated standard deviation in both measurements is very high even though the sample is polished to 30 min. This fact evidence that the polishing time is not enough to achieve a completely flat surface, since some parts of the specimen still have grinding effects in concordance with the FESEM micrographs presented in Figs. 2 and 3.

This observation highlight that by polishing a ground WC-Co during 30 min, the compressive residual layer induced is only partially removed in concordance with Refs. [2,3]. These studies evaluated the residual stresses generated during grinding process by X-Ray diffraction using Cu-K_α radiation and observed that the maximum value is around -2 GPa just on the surface, and it progressively decrease in the subsurface until 12 µm in depth where de compressive residual stresses are in the order of several hundreds of MPa. That means, that two different regions are clearly present in the WC-Co specimens after a ground process; (1) a damaged layer ranging between 200 to 400 nm with a high content of smashed WC particles and cavities and (2) a region where slightly decreases the induced compressive residual stresses due to the amount of plastic deformation events (i.e. dislocations, phase transformation, etc.) mainly located in the metallic Co binder decreases in depth. In that sense, the difference in hardness values obtained between AR and polished samples corresponds to affected sub-layer by grinding visual damage.

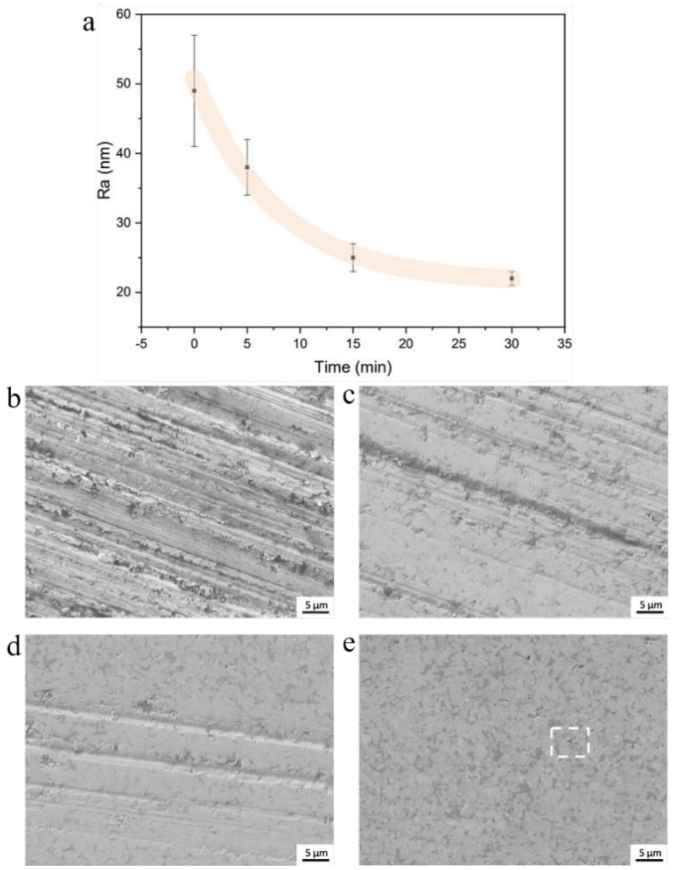

Fig. 2. (a) Roughness evolution as a function of dry-electropolished time. FESEM micrographs of the different WC-Co studied here as a function of the polishing time; (b) AR; (c) after being polished for 5 min; (d) 15 min; and (e) 30 min.

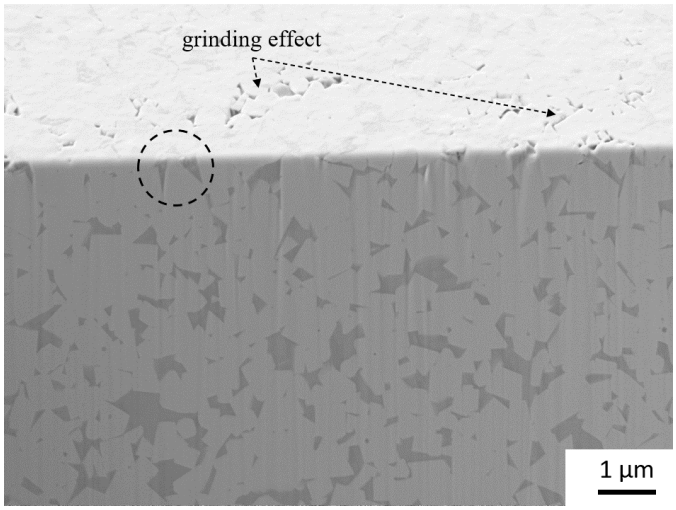

Fig. 3. FIB cross-section micrograph for the speciment polished with DryLyte® tecnhology for 30 min.

However, the reported hardness and elastic modulus presented in Fig. 4 are in agreement with those reported in the literature [17,18] (see grey area marked in the graphs), concluding that DryLyte® process does not modify surface mechanically or chemically of WC-Co sample.

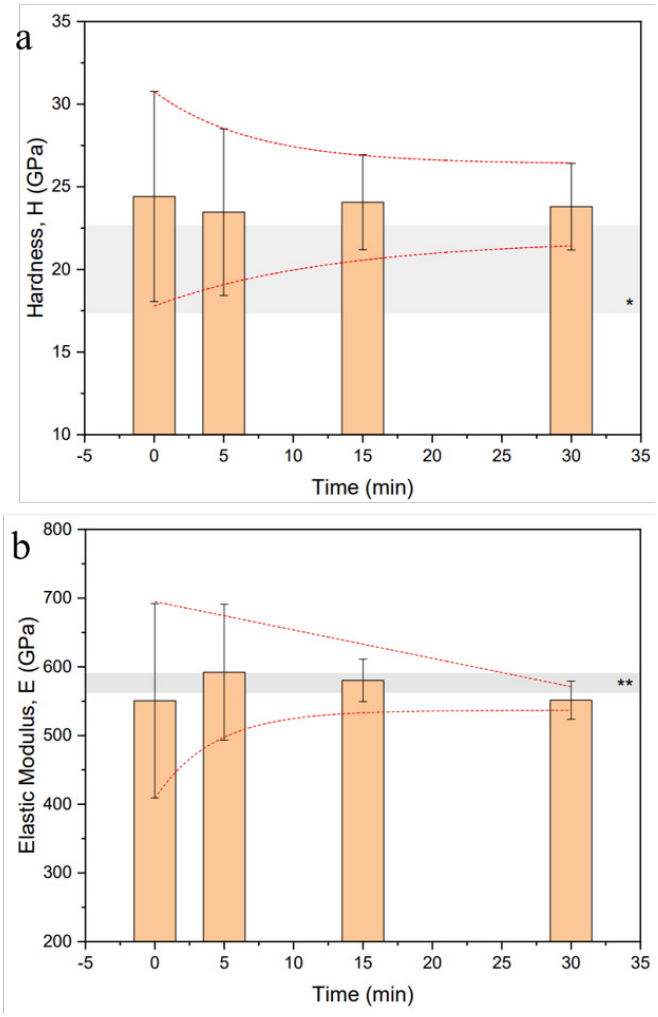

Fig. 4. (a) Hardness; and (b) elastic modulus evolution as a funtion of DryLyte® process time.* and ** corresponds to literature values of hardness and elastic modulus respectively [17,18].

3.3. Correlation between microstructure and mechanical properties

In order to correlate the microstructural features with the mechanical properties, hardness and elastic modulus cartography maps were performed and subsequently the different parameters statistically treated by using the Ulm and Constantinides method [19-21] (more information is available in Appendix A). Fig. 5 exhibits the hardness and elastic modulus cartography as a function of the polishing time. A clear correlation is evident for the AR specimen (see Figs 5a and 5b), where the color difference corresponds to the valleys induced during the grinding process.

Other aspect to take into account, is the dispersion achieved on the results, potentially in AR and during the initial states. That fact is promoted by the damaged scenario that grinding provides at surface level. The surface presents a high roughness value as shown in Fig. 2a being impossible to uniaxially indent the material and obtaining as a consequence a huge scattering of the mechanical values. As the polishing process increases by using the DryLyte® technology, the scatter associated to this measurement and also the amount of scratches decreases, homogenizing the hardness and elastic modulus cartography maps.

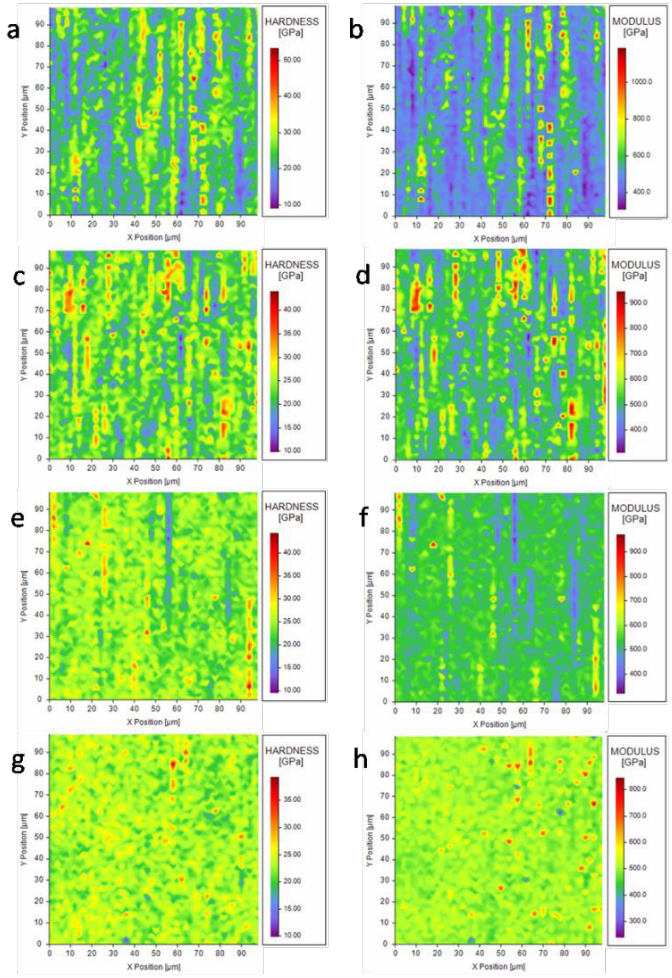

Fig. 5. Hardness (left hand side) and elastic modulus (right hand side) cartography maps evolution as a function of dry-electropolished time (a,b) as-received; (c,d) after being polished for 5 min; (e,f) 15 min; (g,h) 30 min.

Figs. 6a and 6b exhibit the hardness and elastic modulus histograms as well as the deconvoluted peaks (see dash line) after using the statistical method presented in Appendix A for the AR sample. As it can be seen, three and two peaks practically overlapped are clearly visible for the hardness and elastic modulus, respectively. These peaks are not attributed to different constitutive phases, if not due to the different defects induced during the grinding process (i.e., microcracks and nanometric cavities). These defects, generates a superficial roughness which do not lead the Berkovich tip indenter to produce an uniaxial loading. In this particular case, the tip indenter also is affected laterally by the roughness, producing a wide range of values for both mechanical parameters investigated here; hardness (from 8 up to 35 GPa) and elastic modulus (ranging from 250 to 750 GPa). On the other hand, when the polishing process increases up to 15 min (Figs. 6e and 6f), the preliminary peaks disappear (related to the pre-existing defects like particles smash and cavities), showing a main peak

corresponding to the bulk material. In addition, Gaussian simulation for longer polished times shows a decrease in standard deviation until reaching and homogeneous hardness and elastic modulus value of around 23.1 ± 2.5 and 507 ± 42 GPa.

These results highlight that the applied load in this research is too high in order to evaluate the hardness and elastic modulus for each constitutive phase, the anisotropy of WC particles and interactions with the binder, due to the microstructure it has.

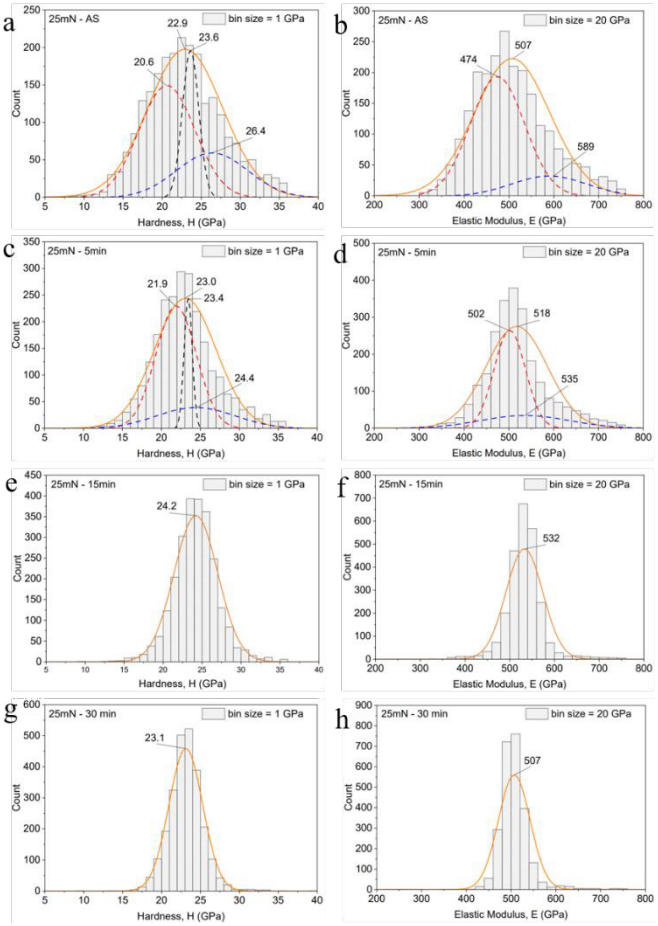

Fig. 6. Hardness (left hand side) and elastic modulus (right hand side) histogram with 1 and 20 GPa of bin size, respectively. Deconvolution as a function of dry-electropolished time for the (a,b) AR sample; (c,d) after being polished for 5 min; (e,f) 15 min; (g,h) 30 min.

4. Conclusions

In this study, the correlation between microstructure and mechanical surface integrity has been evaluated after different dry-electropolishing times at the micro- and submicrometric length scale. In doing so, advanced characterization techniques were used. Based on the research carried out and the results obtained, the following conclusions may be drawn:

- DryLyte® technology allows to polish WC-Co, reducing roughness and removing post-processing defects such as pulverized WC grains and/or smeared Co phase. In addition, not present leaching effect of the metallic Co binder is observed.
- A reduction of the pre-existing grinding effects decreases during the initials 15 min. However, surface integrity in terms of hardness and elastic modulus has still affection along the entire polishing times investigated here.
- Nanoindentation tests show a clear correlation between microstructure and mechanical properties in terms of hardness and elastic modulus. Obtaining stable results by increasing dry-electropolishing time and as a consequence reducing the pre-existing defects at surface level. However, the applied load is too high and the deformation field induced during the indentation process is not possible to be confined in each constitutive phase and consequently it was not possible to extract the hardness and elastic modulus for each one.

Appendix A. Statistical method

A large data from indentations arrays was analysed and subsequently deconvoluted by approximating the distribution of the mechanical properties (p_i) to a Gaussian distribution, described by the following expression:

$$p_i = \frac{1}{\sqrt{2\pi\sigma_i^2}} \exp\left(-\frac{(x-\mu_i)^2}{2\sigma_i^2}\right) \quad (1)$$

where σ_i is standard deviation and μ_i is the arithmetic mean value of hardness (H) and elastic modulus (E) for all indentation N_i in the phase i.

Mean values of μ_i and σ_i were acquired from fitting the cumulative distribution function (CDF) using a sigmoidal shape error function, writing as follows [22,23]:

$$CDF = \sum_{i=1}^{i=n} \frac{1}{2} f_i \left(1 + \operatorname{erf}\left(\frac{x-\mu_i}{\sigma_i\sqrt{2}}\right)\right) \quad (2)$$

where $\sum_{i=1}^{1=n} f_i = 1$. The fitting process was programmed to be completed when the chi-square tolerance (χ^2) is less than $1 \cdot 10^{-15}$.

References

[1] García J, Collado Ciprés V, Blomqvist A, Kaplan B. Cemented carbide microstructures: a review. IntJRefract Met Hard Mater 2019;80:40–68.
[2] Hegeman JBJW, De Hosson JThM, De With G. Grinding of WC-Co hardmetals. Wear 2001;248:187-196.
[3] Yang J, Odén M, Johansson-Jõesaar MP, Llanes L. Grinding effects on surface integrity and mechanical strength of WC-Co cemented carbides. Procedia CIRP 2014;13:257-63.
[4] Yang J, Roa JJ, Odén M, Johansson-Joesaar MP, Llanes L. 3D FIB/FESEM tomography of grinding-induced damage in WC-Co cemented carbides. Procedia CIRP 2020;87:385-390.
[5] Engqvist H, Beste U, Axén N. Influence of pH on sliding wear of WC-based materials. Int J Refract Met Hard Mater 2000;18no.2:103–109.
[6] Pugsley VA, Sockel HG. Corrosion fatigue of cemented carbide cutting tool materials. Mater Sci Eng A 2004;366no.1:87–95.
[7] Human AM, Exner HE. The relationship between electrochemical behaviour and in-service corrosion of WC based cemented carbides. Int J Refract Met Hard Mater 1997;15no.1–3:65–71.
[8] Zhang L, Chen Y, Wan QL, Liu T, Zhu JF, Tian W. Electrochemical corrosion behaviors of straight WC-Co alloys: Exclusive variation in grain sizes and aggressive media. Int J Refract Met Hard Mater 2016;57:70–77.

[9] P202130985. Sarsanedas M, Riu G, Roa JJ. Medio electrolítico para electropulido y método de electropulido con dicho medio 2021.
[10] Oliver WC, Pharr GM. Measurement of hardness and elastic modulus by instrumented indentation: Advances in understanding and refinements to methodology. J Mater Res 2004;19no.1:3–20.
[11] Oliver WC, Pharr GM. An improved technique for determining hardness and elastic modulus load and displacement sensing indentation experiments. Mater Res Soc 1992;7no.6:1564–1583.
[12] Basu S, Moseson A, Barsoum MW. On the determination of spherical nanoindentation stress-strain curves. J Mater Res 2018;21:2628-2637.
[13] Roa JJ, Mateo AM, Llanes L. Implementation of massive nanoindentation coupled with statistical analysis to evaluate complex heterogeneous microstructures in materials manufactured following powder metallurgy processing routes. In: Francisca G Caballero, editor. Encyclopedia of materials: Metals and alloys. Elsevier Inc; 2022;3. p. 465-470.
[14] Tarragó JM, Coureaux D, Torres Y, Wu F, Al-Dawery I, Llanes L. Implementation of an effective time-saving two-stage methodology for microstructural characterization of cemented carbides. Int J Refract Met Hard Mater 2016;55:80–86.
[15] Roebuck B, Almond EA. Deformation and fracture processes and the physical metallurgy of WC–Co hardmetals. Int Mater Rev 1988;33:90–110.
[16] Lee HC, Gurland J. Hardness and deformation of cemented tungsten carbide. Mater Sci Eng 1978;33:125–133.
[17] Roa JJ, Jiménez-Piqué E, Verge C, Tarragó JM, Mateo A, Fair J, Llanes L. Intrinsic hardness of contitutive phases in WC-Co composites: Nanoindentation testing, statistical analysis, WC crystal orientation effects and flow stress for the constrained metallic binder. J Eur Ceram Soc 2015;35:3419-25.
[18] Sandoval DA, Rinaldi A, Notargiacomo A, Ther O, Tarrés E, Roa JJ, Llanes L. Influence of specimen size and microstructure on uniaxial compression of WC-Co micropillars. Ceram Int 2019;45:15934-15941.
[19] Ulm F, Vandamme M, Bobko C, Ortega JA. Statistical indentation technique for hydrated nanocomposites: concrete, bone and shale. J Am Ceram Soc 2007;9:2677-2692.
[20] Constantinides G, Chandran KSR, Ulm F, Van Vliet KJ. Grid indentation analysis of composite microstructure and mechanics: Principles and validation. Mater Sci Eng A 2006;430:189-202.
[21] Constantinides G, Ulm F, Van Vliet K. On the use of nanoindentation for cementitious materils. Mater Struct 2003;36:191-196.
[22] Rayón E, Bonache V, Salvador MD, Roa JJ, Sanchez E. Hardness and Young's modulus distributions in atmospheric plasma sprayed WC-Co coatings using nanoindentation. Surf Coatings Technol 2011;205:4192-4197.
[23] Roa JJ, Jiménez-Piqué E, Tarragó JM, Zivcec M, Broeckmann C, LLanes L. Berkovich nanoindentation and deformation mechanisms in hardmetal binder-like cobalt alloy. Mater Si Eng A 2015;621:128-132.